

Computing excited states of molecules using normalizing flows

Yahya Saleh,^{1,2,*} Álvaro Fernández Corral,^{1,3} Armin Iske,² Jochen Küpper,^{1,3,4} and Andrey Yachmenev^{1,4,†}

¹*Center for Free-Electron Laser Science CFEL, Deutsches*

Elektronen-Synchrotron DESY, Notkestr. 85, 22607 Hamburg, Germany

²*Department of Mathematics, Universität Hamburg, Bundesstr. 55, 20146, Hamburg, Germany*

³*Department of Physics, Universität Hamburg, Luruper Chaussee 149, 22761 Hamburg, Germany*

⁴*Center for Ultrafast Imaging, Universität Hamburg, Luruper Chaussee 149, 22761 Hamburg, Germany*

(Dated: 2023-09-01)

We present a new nonlinear variational framework for simultaneously computing ground and excited states of quantum systems. Our approach is based on approximating wavefunctions in the linear span of basis functions that are augmented and optimized *via* composition with normalizing flows. The accuracy and efficiency of our approach are demonstrated in the calculations of a large number of vibrational states of the triatomic H₂S molecule as well as ground and several excited electronic states of prototypical one-electron systems including the hydrogen atom, the molecular hydrogen ion, and a carbon atom in a single-active-electron approximation. The results demonstrate significant improvements in the accuracy of energy predictions and accelerated basis-set convergence even when using normalizing flows with a small number of parameters. The present approach can be also seen as the optimization of a set of intrinsic coordinates that best capture the underlying physics within the given basis set.

Recently, there has been a significant research interest in employing neural networks to approximate solutions of partial differential equations in general [1–3] and Schrödinger equations specifically [4–6]. These methods proved to mitigate or even break the curse of dimensionality [7, 8] often encountered in standard numerical approximation schemes such as spectral methods or finite volumes. In applications to quantum mechanics, neural networks were employed for computing ground states of spin systems [9], molecular electronic [10, 11] and vibrational states [12, 13]. In most of these methods, many-body wavefunctions are represented by a specially constructed neural network with appropriate symmetry properties, such as the antisymmetry upon the exchange of two electrons. The neural-network parameters are determined by minimizing the energies using variational quantum Monte-Carlo methods (QMC). The combination of the dimension-independent scaling of QMC integration methods with the neural networks’ ability to scale efficiently with the dimension of the problem initiated the development of efficient computational protocols for solving differential equations [1, 3, 4]. Some of these protocols are capable of achieving sub-chemical accuracy for many-electron systems [14].

The majority of neural-network-based QMC methods for solving the Schrödinger equation focused on approximating ground-state solutions. Extensions to excited states are possible by softly enforcing an orthogonality constraint on all lower-energy states *via* a penalty function [15, 16]. Additionally, leveraging the symmetry of the system enables the calculation of excited states as the lowest-energy states within distinct irreducible representations [17]. Although excited-state QMC calculations showed to provide a reasonable balance between accuracy and computational cost [16], their precision and efficiency

are still much lower than those achieved in ground-state QMC calculations, and the accuracy deteriorates with increasing the number of target excited states [16]. Moreover, neural-network-based QMC methods require complex architectural design, good initialization parameters, and constraints on the learning algorithm to reliably compute excited states, particularly for systems with degenerate states [18]. These factors limit the applications of present neural-network approaches to only ground and a few excited states.

In the context of the nuclear motion problem, such as calculations of molecular rovibrational states and spectra, it is essential to compute dozens or even hundreds of excited states with a high level of accuracy [19]. Standard calculations to this end are based on spectral methods [20], where approximate solutions are constructed in the linear span of some basis sets of L^2 , i.e., of square integrable functions. Such methods become increasingly prohibitive as the number of target excited states increases. There are only few studies that used neural networks to calculate excited vibrational states [12, 13], e.g., a single-hidden-layer network for water [12]. The existing studies were limited to computing only a few lowest vibrational states with an accuracy of a few cm⁻¹ and accurately approximating many excited states employing neural networks remains a challenging problem.

Here, we present a new approach to address this problem. In analogy to the use of normalizing flows [21, 22] for augmenting the expressivity of base probability distributions, we propose to augment the expressivity of basis sets of L^2 *via* composition with invertible neural networks [23]. We introduce a nonlinear ansatz that represents ground and excited wavefunctions in the linear span of such augmented basis sets, where we optimize the parameters of the neural network using the varia-

tional principle. We demonstrate the capability of this approach to efficiently and accurately compute dozens of molecular vibrational and electronic excited states using relatively modest basis sets, even when small invertible neural networks are employed. Moreover, we numerically show that such calculations converge rapidly as the size of the truncated basis increases. For numerical tests, we computed vibrational states of the H_2S molecule as well as electronic states of one-electron systems including the hydrogen atom, the molecular hydrogen ion, and a carbon atom in a single-active-electron approximation.

We start by choosing an appropriate truncated set of basis functions $\{\phi_n(r)\}_{n=1}^N$ of L^2 and an invertible neural network g_θ parameterized by a set of parameters θ that maps a coordinate vector r to a vector q of the same dimension. We then define the augmented set of functions $\{\phi_n^{(A)}(r; \theta)\}_{n=1}^N$ as follows

$$\phi_n^{(A)}(r; \theta) := \phi_n(g_\theta(r)) \sqrt{|\det \nabla_r g_\theta(r)|}, \quad (1)$$

where the square root of the determinant of the Jacobian ensures the orthonormality of the augmented functions with respect to the L^2 -inner product regardless of the values of θ , assuming the original basis set is orthonormal. In addition to orthonormality, it can be demonstrated that the augmented functions $\{\phi_n^{(A)}\}_{n=1}^N$ also form a complete basis in L^2 in the limit of $N \rightarrow \infty$ [24].

We approximate the wavefunctions for the ground and excited states $\Psi_m(r)$, $m = 1 \dots M$, of a molecular system in the linear span of augmented basis functions, i. e.,

$$\Psi_m(r) \approx \sum_{n \leq N} c_{nm} \phi_n^{(A)}(r; \theta). \quad (2)$$

For fixed values of the parameters θ , the linear expansion coefficients $\mathbf{C} = \{c_{nm}\}_{n,m}^{N,M}$ and the corresponding state energies $\mathbf{E} = \{E_m\}_m^M$ are determined by solving the eigenvalue problem

$$\mathbf{E} = \mathbf{C}^{-1} \mathbf{H} \mathbf{C}, \quad (3)$$

where $\mathbf{H} = \mathbf{T} + \mathbf{V}$ is the sum of matrix representations of the kinetic and potential energy operators in the augmented basis. By introducing a change of variables $q = g_\theta(r)$, the expressions for the matrix elements of the kinetic and potential energy operators can be written

as follows

$$T_{nn'} = -\frac{\hbar^2}{2} \sum_{\lambda, \mu} \int \phi_n^*(q) G_{\lambda\mu}(g_\theta^{-1}(q)) \quad (4)$$

$$\begin{aligned} & \times \left\{ \sum_{k,l} \frac{\partial q_k}{\partial r_\lambda} \frac{\partial q_l}{\partial r_\mu} \frac{\partial^2}{\partial q_k \partial q_l} + \sum_k \frac{\partial^2 q_k}{\partial r_\lambda \partial r_\mu} \frac{\partial}{\partial q_k} \right. \\ & + \frac{1}{2} \sum_k \left(\frac{\partial q_k}{\partial r_\lambda} \frac{\partial D}{\partial r_\mu} + \frac{\partial q_k}{\partial r_\mu} \frac{\partial D}{\partial r_\lambda} \right) \frac{1}{D} \frac{\partial}{\partial q_k} \\ & \left. - \frac{1}{4} \frac{\partial D}{\partial r_\lambda} \frac{\partial D}{\partial r_\mu} \frac{1}{D^2} + \frac{1}{2} \frac{\partial^2 D}{\partial r_\lambda \partial r_\mu} \frac{1}{D} \right\} \phi_{n'}(q) dq, \\ V_{nn'} &= \int \phi_n^*(q) V(g_\theta^{-1}(q)) \phi_{n'}(q) dq. \end{aligned} \quad (5)$$

Here, $D = |\det \nabla_r g_\theta(r)|$, $G_{\lambda\mu}$ is the kinetic-energy matrix, λ, μ indices are used to denote the elements of the coordinate vector r , and k, l indices denote the elements of the coordinate vector q , i. e., $q_k = g_{\theta,k}(r)$ and $r_\lambda = g_{\theta,\lambda}^{-1}(q)$.

The linear-expansion coefficients c_{nm} and the parameters θ of the normalizing flow g_θ can be optimized using the variational principle, that is, by minimizing the energies of the ground and excited states. Here, we use the sum of all energies spanned by the basis as the loss function, i. e.,

$$\mathcal{L}_\theta = \sum_{m \leq M} E_m = \text{Tr}(\mathbf{H}) \rightarrow \min_\theta. \quad (6)$$

One of the advantages of the loss function in (6) is its relatively low computational cost, as it requires the evaluation of only the diagonal elements of the Hamiltonian matrix when the initial basis is orthonormal. Moreover, given the invariance of the matrix trace function under unitary transformations, the optimization of the parameters θ is decoupled from the eigenvector coefficients c_{nm} , which further improves the computational efficiency. This is different when the loss function takes the sum of only the few lowest eigenvalues spanned by the basis. In this case, the sum will depend on the eigenvector coefficients c_{nm} , which will require a repeated solution of the eigenvalue problem during the optimization of the parameters θ . However, despite the added complexity, the high accuracy achieved even with modest-size basis sets can outweigh the computational costs of the repeated matrix diagonalization.

One of the most computationally expensive parts of this approach is the calculation of the integrals in (4) and (5). We employed Gaussian quadratures, altering the quadrature degree at different optimization steps to avoid overfitting. We found that alternating between smaller quadratures during optimization was computationally more efficient and converging to approximately the same values of parameters θ as those obtained using a fixed large quadrature. After convergence, the final energies

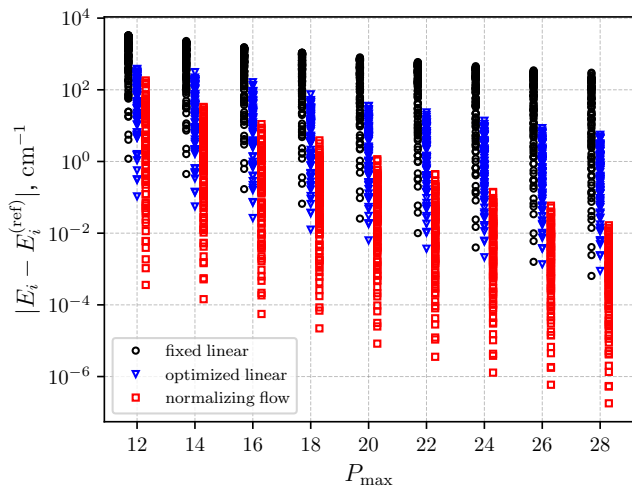


FIG. 1. Convergence of the lowest one hundred vibrational energies of H_2S , E_i ($i = 1..100$), plotted against the size of the truncated vibrational basis set, defined by the polyad number P_{\max} . Results obtained with fixed-linear (black circles), optimized-linear (blue triangles), and normalizing-flow (red squares) parameterizations are compared. The energies for fixed-linear and normalizing-flow parameterizations are shifted left and right from the polyad number value, respectively, for visual clarity. The reference energies $E_i^{(\text{ref})}$ were obtained from normalizing-flow calculations with $P_{\max} = 32$.

and wavefunctions were calculated by solving the eigenvalue problem in (3) using a large quadrature for accurate evaluation of the integrals. In order to further decrease the cost of numerical integration, especially in multidimensional problems, other strategies such as sparse-grid approaches [25], collocation [26], or Monte-Carlo [18, 27] can be employed.

The accuracy and performance of our approach was tested in calculations of vibrational states of H_2S and electronic states of prototypical one-electron systems. For H_2S , we solved a fully-coupled three-dimensional vibrational problem with a spectroscopically refined potential energy surface [28]. For the electronic problems, we only considered the normalizing flows for the radial coordinate and integrated out the angular coordinates using the spherical-harmonic basis. The details of the Hamiltonian construction and variational computations are provided in the supplementary material.

To model the normalizing flow g_θ , we used the invertible residual neural network of the form: $g_\theta(x) = a(x + K_\theta(x)) + b$, where a and b are constants representing a linear scaling and shift of the input and K_θ is a standard multilayer perceptron, e.g., $K_\theta = W_n\phi(W_{n-1}\phi(W_{n-2}\phi(\dots) + B_{n-2}) + B_{n-1}) + B_n$ with multiple linear layers (W_i, B_i) and nonlinear activations ϕ . The invertibility of the residual block is imposed by requiring that the Lipschitz constant for the block is strictly lower than one [29], i.e., $\text{Lip}(K_\theta) =$

$\max_{\{x,y\}} |(K_\theta(x) - K_\theta(y))/(x - y)| < 1$. As demonstrated in [29], this can be achieved by using spectral normalization for each of the dense layers in the multilayer network $K_\theta(x)$, i.e., $W_i \rightarrow W_i/\|W_i\|_2$, where $\|W_i\|_2$ is calculated using singular value decomposition of the Fourier-transformed matrix [30]. To avoid the derivative-saturation problem, which ultimately leads to loss of the expressive power of the network, a few special activation functions were proposed in the literature, such as LipSwish(x) = $x\sigma(x)/1.1$ [31] and its concatenated form [32]. Further details of the residual neural network and its optimization are provided in supplementary material.

We used Hermite functions as a basis of L^2 for solving both the vibrational and electronic radial problems. In the case of H_2S , the basis set was composed of the direct product of Hermite functions $H_{n_i}(\xi_i)e^{-\xi_i^2/2}$ associated with each of the vibrational coordinates $\xi_1, \xi_2, \xi_3 = r_{\text{SH}_1}, r_{\text{SH}_2}, \alpha_{\angle \text{H}_1\text{SH}_2}$, where H_{n_i} is the n_i -th order Hermite polynomial. The basis set was truncated such that the maximal value of the polyad number, P_{\max} , satisfied the condition $P_{\max} \geq 2n_1 + 2n_2 + n_3$. For the electronic radial problem, the basis-set size was determined solely by the maximum number of Hermite functions, denoted as N_{\max} .

FIG. 1 illustrates the convergence of the lowest one hundred vibrational energies of H_2S as a function of the basis-set size, characterized by P_{\max} . The results obtained from normalizing-flow calculations are compared with the standard approach that employs a linear parametrization of the coordinates, namely $q_i = a_i\xi_i + b_i$. The values of the linear parameters a_i and b_i are chosen such that the one-dimensional Hamiltonian of q_i best matches that of a harmonic oscillator. That is, $a_i = (G_{ii}/(2\omega_i))^{1/4}$ and $b_i = \xi_i^{(\text{eq})}$, where G_{ii} is the diagonal element of the kinetic energy matrix and the $\omega_i = \partial^2 V/\partial \xi_i^2$ are evaluated at the equilibrium geometry $\xi_i^{(\text{eq})}$. Such a coordinate transformation is commonly used in variational calculations of vibrational energies and works well for potentials V close to a harmonic function. For anharmonic potentials, the linear parameters can be further optimized using the same computational procedure as proposed above for optimizing normalizing flows. The vibrational energies calculated with the optimized-linear parametrization are also shown in FIG. 1.

The results clearly show that energies obtained using basis functions augmented with a normalizing flow are more accurate for any size of the truncated basis. Moreover, the normalizing-flow parametrization yields a significantly faster basis-set convergence than both the fixed-linear and the optimized-linear ones. At $P_{\max} = 28$, the accuracy achieved using a normalizing flow exceeds that of the optimized-linear and fixed-linear parametrizations by nearly three and five orders of magnitude, respectively. In order to achieve a comparable accuracy with a direct-

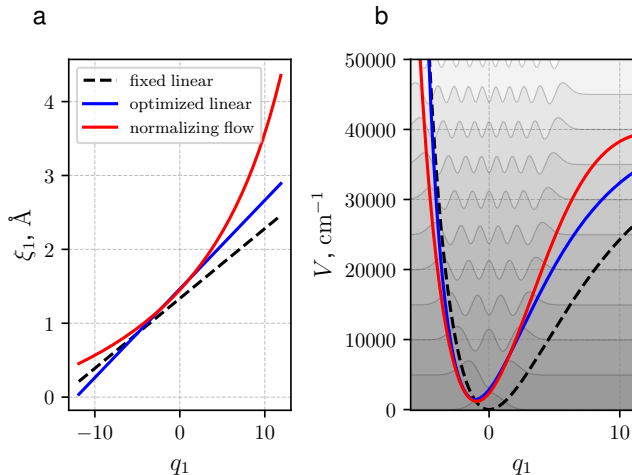


FIG. 2. (a) The S-H vibrational stretching coordinate $\xi_1 = g_{\theta,1}^{-1}(q_1, q_2, q_3)$ and (b) the potential energy $V(q_1, q_2, q_3)$ of H_2S , plotted as function of q_1 , with $q_2 = q_3 = 0$, for the fixed-linear (dashed black), optimized-linear (solid blue), and normalizing-flow (solid red) parameterizations. As visual aids, Hermite functions, which are solutions of the harmonic approximation to $V(q_1, q_2, q_3)$, ranging from 0 to 20 in increments of 2 are plotted as shaded regions.

product basis set and fixed-linear parametrization, we estimate that a basis with $P_{\max} > 80$ would be necessary, which is computationally unfeasible. Notably, the computational effort required for optimizing the linear and normalizing-flow parametrizations utilized in this work is comparable, with a slight computational overhead for the normalizing flow backpropagation. The calculated vibrational energies match the results of previous calculations using the variational approach TROVE [28] within $< 1 \text{ cm}^{-1}$. The remaining discrepancies arise from the neglected pseudopotential operator in our simulations, see the supplementary information.

To visualize the effect of the normalizing flow we plot one-dimensional cuts of the coordinate transformations along the q_1 coordinate ($q_2 = q_3 = 0$) in FIG. 2 for the fixed-linear, optimized-linear, and normalizing-flow parametrizations obtained with $P_{\max} = 20$. We found that the optimized normalizing-flow function g_{θ} does not couple different input coordinates much, which is why only a single output value corresponding to the ξ_1 stretching coordinate is plotted as a function of q_1 . Corresponding plots for other coordinates are shown in the supplementary information. The resulting potential energy curves are plotted in FIG. 2 b. Clearly, the optimized-linear parametrization produces a slight scaling and shifting of the potential, enabling a more effective coverage by the Hermite basis functions, as depicted by the shaded areas in FIG. 2 b. This leads to an improved representation of excited states. This effect is even more pronounced in the case of the normalizing flow, which further modi-

fies the shape of the potential to better encompass basis functions, resulting in a closer alignment with a harmonic-oscillator potential. Thus, approximating wavefunctions in the linear span of augmented functions can be viewed as a means of identifying an optimal set of coordinates, $q = g_{\theta}(r)$, which transforms the original Hamiltonian, e.g., the potential $V(g_{\theta}^{-1}(q))$ in (5), to closely resemble the Hamiltonian for which the selected basis set forms a set of eigenfunctions. Using a nonlinear parameterization, such as the one presented by a normalizing flow, is more efficient for this purpose than linear parameterizations.

The application of the Hermite basis set composed with a normalizing-flow function also demonstrates high accuracy and fast basis-set convergence for the radial electronic problem, although such basis is typically considered unsuitable for solving electronic problems. FIG. 3 shows the convergence of the electronic-state energies for H, H_2^+ , and C as a function of the radial Hermite-basis size N_{\max} . The results are compared against the linear parametrization, $q = ar + b$, where the constants a and b were optimized. Using the normalizing-flow approach, the electronic energies of H and H_2^+ converge very quickly to within 10^{-3} hartree of the exact and reference *ab initio* values for the ground state, respectively, and even more precisely for the excited states. The accuracy for H_2^+ is constrained to $\sim 10^{-3}$ hartree due to truncation in the Laplace expansion of the nuclear-attraction potential. When employing linear parametrization, considerably larger Hermite basis sets would be required to reach acceptable convergence. For further information, tables with the calculated excited-state energies and plots of the optimized-linear and normalizing-flow parametrizations for the electronic radial coordinate together with the corresponding potentials are provided in the supplementary information. The coordinate and potential plots demonstrate the same behavior as in the case of the H_2S vibrations, namely that the optimization modifies the potential to more effectively encompass Hermite basis functions, which is more pronounced for the ground electronic state.

In the present approach, we compose standard basis sets of L^2 with normalizing flows and use the resulting functions to approximate molecular wavefunctions. We demonstrate its high accuracy and fast basis-set convergence in calculations of ground and large number of excited vibrational and electronic states of molecules. In contrast to other neural network approaches, the present method does not suffer from convergence issues during nonlinear optimization. We attribute this to the strong inductive bias obtained by employing an initial basis set of L^2 , as well as the retained property of completeness for basis sets composed with standard implementations of normalizing flows, such as invertible residual networks [33]. Other more architecturally-complex neural-network methods [6, 11, 16] are more limited in their calculations of excited states, so the present method has the potential

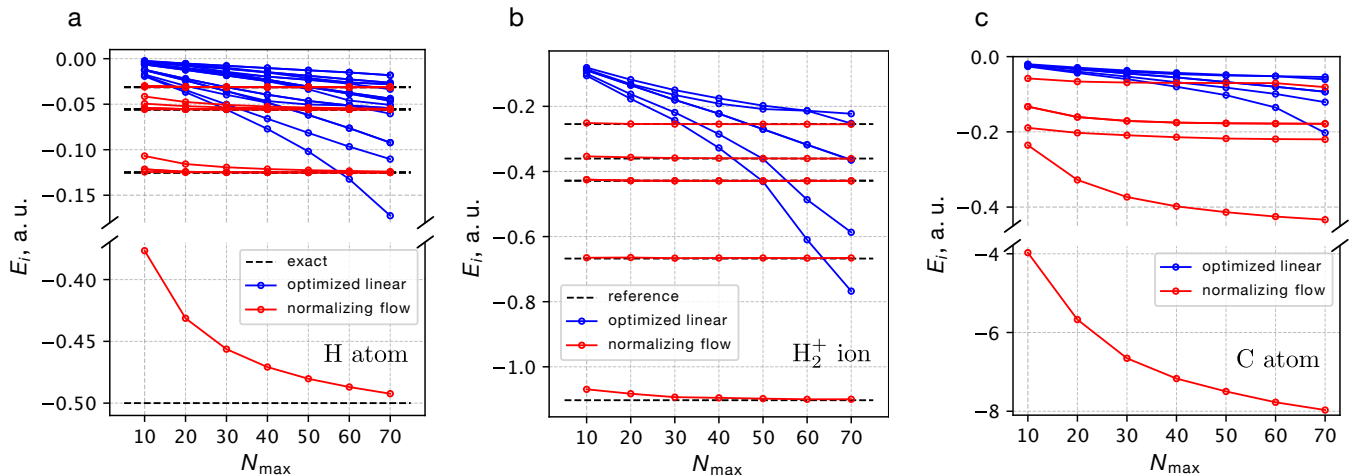


FIG. 3. Convergence of the electronic ground- and excited-state energies of (a) the hydrogen atom, (b) the molecular hydrogen ion H_2^+ , and (c) the carbon atom as a function of the number of Hermite radial basis functions N_{max} . Results obtained with optimized-linear (solid blue) and normalizing-flow (solid red) parameterizations are compared. The exact energies for the hydrogen atom and reference configuration-interaction energies in the aug-cc-pV5Z basis set for H_2^+ are depicted as dashed black lines.

to significantly improve the methodology, in particular for excited electronic states when extended to account for electron correlation.

The present method can also be viewed as a technique for determining an optimal set of intrinsic coordinates that best characterize the problem of interest. By developing and employing nonlinear parametrizations that can reduce the dimensionality of the original coordinate space, such as canonical embeddings of homeomorphisms [34], one can optimize a reduced set of coordinates that capture the very essence of the underlying process, thereby reducing the complex molecular dynamics to a few effective key degrees of freedom [35].

We believe that the current method can be straightforwardly applied to the computations of highly-excited vibrational states of molecules and has the potential for computations of resonance and predissociation states, where the requirements to basis set convergence are extremely tight [36]. For the electronic problem, the extension to account for electron correlation is possible using appropriate numerical integration schemes, such as Monte-Carlo methods.

We thank Jannik Eggers, Sebastian Nicolas Mendoza, and Vishnu Sanjay for useful comments and discussions in early stages of this work. This work was supported by Deutsches Elektronen-Synchrotron DESY, a member of the Helmholtz Association (HGF), including the Maxwell computational resource operated at DESY, by the Data Science in Hamburg HELMHOLTZ Graduate School for the Structure of Matter (DASHH, HIDSS-0002), and by the Deutsche Forschungsgemeinschaft (DFG) through the cluster of excellence “Advanced Imaging of Matter” (AIM, EXC 2056, ID 390715994).

* Email: yahya.saleh@cfel.de

† Email: andrey.yachmenev@cfel.de;

URL: <https://www.controlled-molecule-imaging.org>

- [1] W. E and B. Yu, The deep Ritz method: a deep learning-based numerical algorithm for solving variational problems, *Commun. Math. Stat.* **6**, 1 (2018).
- [2] E. Kharazmi, Z. Zhang, and G. E. Karniadakis, Variational physics-informed neural networks for solving partial differential equations, (2019), arXiv:1912.00873 [cs].
- [3] W. E, J. Han, and A. Jentzen, Deep learning-based numerical methods for high-dimensional parabolic partial differential equations and backward stochastic differential equations, *Comm. Math. Stat.* **5**, 349 (2017).
- [4] J. Han, J. Lu, and M. Zhou, Solving high-dimensional eigenvalue problems using deep neural networks: A diffusion Monte Carlo like approach, *J. Comput. Phys.* **423**, 109792 (2020).
- [5] J. Kessler, F. Calcavecchia, and T. D. Kühne, Artificial neural networks as trial wave functions for quantum Monte Carlo, *Adv. Theory Simul.* **4**, 2000269 (2021).
- [6] J. Hermann, J. Spencer, K. Choo, A. Mezzacapo, W. Foulkes, D. Pfau, G. Carleo, and F. Noé, Ab-initio quantum chemistry with neural-network wavefunctions (2022), arXiv:2208.12590 [physics].
- [7] M. Hutzenthaler, A. Jentzen, T. Kruse, T. A. Nguyen, and P. von Wurstemberger, Overcoming the curse of dimensionality in the numerical approximation of semilinear parabolic partial differential equations, *Proc. R. Soc. A.* **476**, 20190630 (2020).
- [8] P. Grohs, F. Hornung, A. Jentzen, and P. Von Wurstemberger, A proof that artificial neural networks overcome the curse of dimensionality in the numerical approximation of Black-Scholes partial differential equations (2018), arXiv:1809.02362 [physics].
- [9] G. Carleo and M. Troyer, Solving the quantum many-body problem with artificial neural networks, *Science* **355**, 602

- (2017).
- [10] J. Hermann, Z. Schätzle, and F. Noé, Deep-neural-network solution of the electronic Schrödinger equation, *Nat. Chem.* **12**, 891 (2020).
 - [11] D. Pfau, J. S. Spencer, A. G. D. G. Matthews, and W. M. C. Foulkes, *Ab initio* solution of the many-electron Schrödinger equation with deep neural networks, *Phys. Rev. Research* **2**, 033429 (2020).
 - [12] S. Manzhos, K. Yamashita, and T. Carrington Jr, Using a neural network based method to solve the vibrational Schrödinger equation for H₂O, *Chem. Phys. Lett.* **474**, 217 (2009).
 - [13] S. Manzhos, M. Ihara, and T. Carrington, Machine learning for vibrational spectroscopy, in *Quantum Chemistry in the Age of Machine Learning* (Elsevier, 2023) pp. 355–390.
 - [14] W. Ren, W. Fu, X. Wu, and J. Chen, Towards the ground state of molecules via diffusion Monte Carlo on neural networks, *Nat. Commun.* **14**, 1860 (2023), arXiv:2204.13903 [physics].
 - [15] S. Pathak, B. Busemeyer, J. N. B. Rodrigues, and L. K. Wagner, Excited states in variational Monte Carlo using a penalty method, *J. Chem. Phys.* **154**, 034101 (2021).
 - [16] M. Entwistle, Z. Schätzle, P. A. Erdman, J. Hermann, and F. Noé, Electronic excited states in deep variational Monte Carlo, *Nat. Commun.* **14**, 274 (2023), arXiv:2203.09472 [physics].
 - [17] K. Choo, G. Carleo, N. Regnault, and T. Neupert, Symmetries and many-body excitations with neural-network quantum states, *Phys. Rev. Lett.* **121**, 167204 (2018).
 - [18] A. Cuzzocrea, A. Scemama, W. J. Briels, S. Moroni, and C. Filippi, Variational principles in quantum Monte Carlo: The troubled story of variance minimization, *J. Chem. Theory Comput.* **16**, 4203 (2020).
 - [19] A. G. Császár, T. Furtenbacher, and P. Árendás, Small molecules — big data, *J. Phys. Chem. A* **120**, 8949 (2016).
 - [20] D. Gottlieb and S. A. Orszag, *Numerical analysis of spectral methods: theory and applications* (SIAM, 1977).
 - [21] D. Rezende and S. Mohamed, Variational inference with normalizing flows, in *Proceedings of the 32nd International Conference on Machine Learning, ICML*, Proceedings of Machine Learning Research, Vol. 37, edited by F. Bach and D. Blei (PMLR, 2015) pp. 1530–1538.
 - [22] G. Papamakarios, E. Nalisnick, D. J. Rezende, S. Mohamed, and B. Lakshminarayanan, Normalizing flows for probabilistic modeling and inference, *J. Mach. Learn. Res.* **22**, 2617 (2022).
 - [23] K. Cranmer, S. Golkar, and D. Pappadopulo, Inferring the quantum density matrix with machine learning (2019), arXiv:1904.05903 [physics].
 - [24] Y. Saleh, *Spectral and active learning for enhanced and computationally scalable quantum molecular dynamics*, Dissertation, Universität Hamburg, Hamburg, Germany (2023).
 - [25] G. Avila and T. Carrington, Solving the Schrödinger equation using Smolyak interpolants, *J. Chem. Phys.* **139**, 134114 (2013).
 - [26] W. Yang and A. C. Peet, The collocation method for bound solutions of the Schrödinger equation, *Chem. Phys. Lett.* **153**, 98 (1988).
 - [27] J. Toulouse and C. J. Umrigar, Full optimization of Jastrow-Slater wave functions with application to the first-row atoms and homonuclear diatomic molecules, *J. Chem. Phys.* **128**, 174101 (2008).
 - [28] A. A. A. Azzam, J. Tennyson, S. N. Yurchenko, and O. V. Naumenko, ExoMol molecular line lists – XVI. the rotation-vibration spectrum of hot H₂S, *Mon. Not. R. Astron. Soc.* **460**, 4063 (2016).
 - [29] J. Behrmann, W. Grathwohl, R. T. Q. Chen, D. Duvenaud, and J.-H. Jacobsen, Invertible residual networks, in *Proceedings of the 36th International Conference on Machine Learning*, Proceedings of Machine Learning Research, Vol. 97, edited by K. Chaudhuri and R. Salakhutdinov (PMLR, 2019) pp. 573–582.
 - [30] H. Sedghi, V. Gupta, and P. M. Long, The singular values of convolutional layers, in *International Conference on Learning Representations (ICLR)* (2019) arXiv:1805.10408 [cs].
 - [31] R. T. Q. Chen, J. Behrmann, D. K. Duvenaud, and J.-H. Jacobsen, Residual flows for invertible generative modeling, in *Advances in Neural Information Processing Systems*, Vol. 32, edited by H. Wallach, H. Larochelle, A. Beygelzimer, F. d'Alché-Buc, E. Fox, and R. Garnett (Curran Associates, Inc., 2019) pp. 9916–9926.
 - [32] Y. Perugachi-Diaz, J. Tomczak, and S. Bhulai, Invertible densenets with concatenated LipSwish, in *Advances in Neural Information Processing Systems*, Vol. 34, edited by M. Ranzato, A. Beygelzimer, Y. Dauphin, P. Liang, and J. W. Vaughan (Curran Associates, Inc., 2021) pp. 17246–17257.
 - [33] Y. Saleh, A. Iske, A. Yachmenev, and J. Küpper, Augmenting basis sets by normalizing flows, *Proc. Appl. Math. Mech.* **23**, e202200239 (2023), arXiv:2212.01383 [math].
 - [34] J. Brehmer and K. Cranmer, Flows for simultaneous manifold learning and density estimation, in *Advances in Neural Information Processing Systems, NeurIPS*, Vol. 33, edited by H. Larochelle, M. Ranzato, R. Hadsell, M. Balcan, and H. Lin (Curran Associates, Inc., 2020) pp. 442–453.
 - [35] A. A. Ischenko, P. M. Weber, and R. J. D. Miller, Capturing chemistry in action with electrons: Realization of atomically resolved reaction dynamics, *Chem. Rev.* **117**, 11066 (2017).
 - [36] A. G. Császár, I. Simkó, T. Szidarovszky, G. C. Groenenboom, T. Karman, and A. van der Avoird, Rotational-vibrational resonance states, *Phys. Chem. Chem. Phys.* **22**, 15081 (2020).